# Nanophysics laboratory

N. Lonigro (mat. 1218058)
L. Zampieri (mat. 1237351)

June 21, 2020

The purpose of the laboratory activity is to produce, characterize and model colloidal gold nanoparticles.

## 1 Production

The synthesis of the nanoparticles has been performed following the Turkevich method. A solution of $HAuCl_4$ (1mM, 9.5ml) and a solution of $Na_3C_6H_5O_7$ (95mM, 0.5ml) are separately heated, thanks to a boiling water bath, to the temperature of 100°C. The two solutions are mixed thanks to a mechanical stirrer such that atomic gold is released.

$$2\,HAuCl_4 + 4\,Na_3C_6H_5O_7 \longrightarrow 2\,Au + H_2 + 4\,CO_2 + 4\,NaC_5H_5O_5 + 8\,NaCl$$

Finally, the solution is diluted 1 : 10 in Milli-Q water.

In the limit that all the tetrachloroauric acid goes through the redox reaction, the density of gold atoms is:

$$n_{max} = \frac{1\text{mM} \cdot 9.5\text{ml}}{10\text{ml}} \cdot \frac{1}{10} = 95\mu\text{M} \tag{1}$$

which can be useful as a upper bound in nanoparticles density.

## 2 Optical characterization

The nanoparticles solution is then analyzed using a spectrophotometer, scanning in the wavelengths range $400 - 900$nm. From the theory, we know that in the non-interacting dipolar approximation the absorbance can be written as:

$$\begin{aligned} A &= \log_{10}(e) z \rho \sigma_{ext} \\ &= z\rho R^3 \cdot 9 \log_{10}(e) \frac{\omega}{c} \varepsilon_m^{3/2} \cdot \frac{4}{3}\pi \frac{\varepsilon_2}{(\varepsilon_1 + 2\varepsilon_m)^2 + \varepsilon_2^2} \end{aligned} \tag{2}$$

where $z$ is the couvette thickness ($\approx$ 1cm), $\rho$ is the nanoparticles numerical density, $R$ is the nanoparticles radius, $\omega$ is the incident wave pulsation, $c$ is the light speed, $\varepsilon_m$ is the environment dielectric function and $\varepsilon = \varepsilon_1 + i\varepsilon_2$ is the gold one.

Note that the absorbance depends only by the product $z\rho R^3$ and therefore there is no possibility to separately fit the radius and the density. It's necessary to consider the size dependence of the dielectric function:

$$\varepsilon(R, \omega) = \varepsilon_\infty + \omega_P^2 \left( \frac{1}{\omega^2 + \Gamma_\infty^2} - \frac{1}{\omega^2 + \Gamma_R^2} \right) - i \frac{\omega_P^2}{\omega} \left( \frac{\Gamma_\infty}{\omega^2 + \Gamma_\infty^2} - \frac{\Gamma_R}{\omega^2 + \Gamma_R^2} \right)$$

where $\varepsilon_\infty$ is the bulk gold dielectric function, $\omega_P$ is the plasma frequency, and $\Gamma$ is the scattering frequency, which is size dependent following the relation

$$\Gamma_R = \Gamma_\infty + C \frac{v_F}{R}$$

where $v_F$ is the Fermi speed.

From the literature, the gold bulk dielectric function is known as a function of the frequency (1) while for the other quantities we accepted the following values*, which are provided without errors:

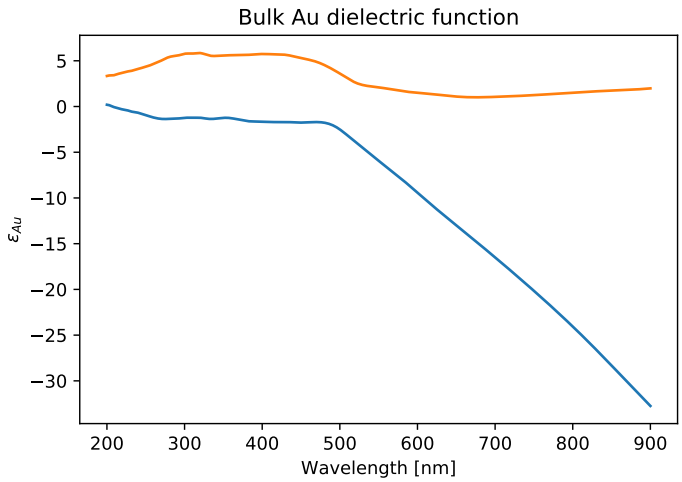


Figure 1: Gold bulk dielectric function

$$\omega_P = 8.557\text{eV} \qquad \Gamma_\infty = 0.072\text{eV}$$
$$C = 0.8 \qquad v_F = 1.41 \cdot 10^6 \text{m/s}$$

Note that, as many articles point out, some of these values are purely indicative. For example, the value of $C$ is not well defined: values from 0.1 to 2 have been theoretically justified*.

Spectra are then simulated and $\chi^2$ is computed varying $\rho$, $R$ and $\varepsilon_m$ in suitable ranges. Fits are performed for $\rho$ between $10^{-4}$ and $10^{-1}$µM, $R$ between 1 and 14nm and $\varepsilon_m$ between $(1.3)^2$ and $(1.5)^2$. The minimum $\chi^2$ is reached for the following combination:

$$R \sim 5\text{nm} \qquad \rho \sim 10\text{nM}$$
$$\varepsilon_m \sim 2.0 \quad (n \sim 1.4)$$

In the following figures, the map of inverse $\chi^2$ are reported sectioning in correspondence of the minimum.

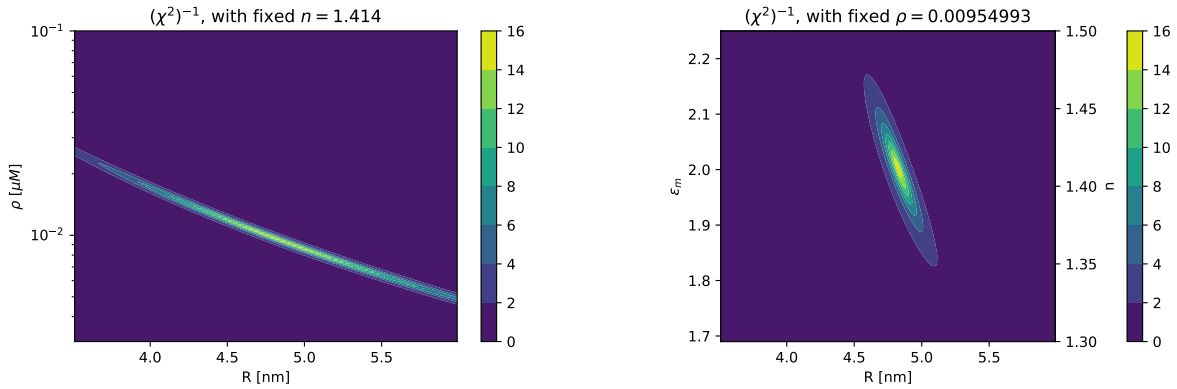


(a) Section in the plane $\rho, R$

(b) Section in plane $\varepsilon_m, R$

Figure 2: Inverse $\chi^2$ maps.

*Scaffardi, Tocho, *Size dependence of refractive index of gold nanoparticles.* Nanotechnology 17, 1309 (2006). `https://doi.org/10.1088/0957-4484/17/5/024`

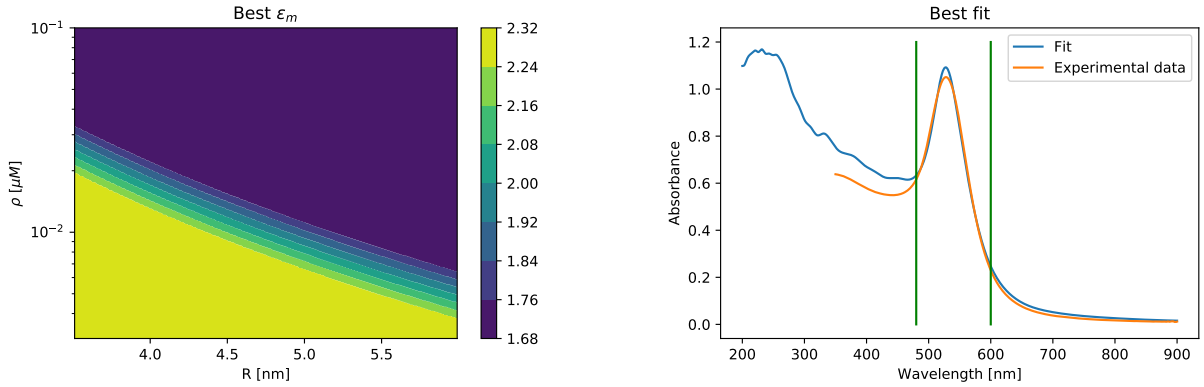


(a) Best $\varepsilon_m$ values for different $(\rho, R)$

(b) Best fit. In green, the fit limits.

Figure 3: Fit results

Regarding the range selected for the fit (fig. 3(b)), the left section of the spectra has been neglected, since effects due to interband transitions appear and our model is not able to describe the cross section anymore. Similarly, the long right tail of the spectra has been neglected, considering only a range around the interesting peak.

From the $\chi^2$ maps it's clear that $R$ and $\rho$ are strongly correlated. For example, as it's clear from plot 2(a), there is an inverse correlation between $R$ and $\rho$, which reflect the dependence from the product $\rho R^3$ in eq. (2). However, comparing plot 2(a) with plot 3(a), can be observed that the estimation of $\varepsilon_m$ is more or less constant around the "stability valley" of the $(\rho, R)$ map. This lead us, considering also the wide uncertainties of the absorbance equation parameters, to not assign an error to the fit results, but to consider them as order of magnitude indications.

From the fit results, the filling fraction can be computed:

$$f = \rho \frac{4}{3} \pi R^3 \sim 2.7 \cdot 10^{-6}$$

This fraction is way lower than 1%: this confirm us that the approximation of non-interacting nanoparticles can be safely applied to the system.

Observe that considering the bulk gold density $\rho^{\infty}_{\text{atom}} \sim 5.9 \cdot 10^{28} \text{atoms/m}^3$, the numerical gold atom density can be roughly estimated as:

$$\rho_{\text{atom}} = \rho \cdot \frac{4}{3} \pi R^3 \cdot \rho^{\infty}_{\text{atom}} \sim 300 \mu\text{M}$$

which is, in order of magnitude, compatible with the estimated one (eq. (1)).

## 3 X-ray diffraction

A sample of gold nanoparticles has been analysed via X-ray diffraction after their deposition on a silicon substrate catalyzed by APTES molecules. The analysis has been performed using an X'Pert Pro diffractometer. A beam of X-ray with $\lambda = 0.15406nm$ has been obtained by electron scattering on a Cu foil and it was used as probe to study the size and structure of the nanoparticles.The spectrum obtained with an incident angle of 0.6° as reported in Fig.4.

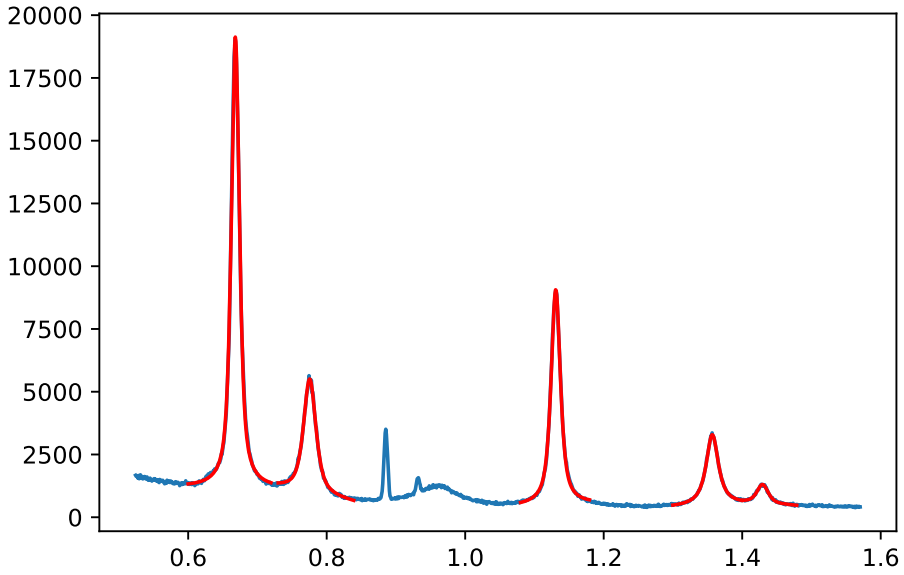


Figure 4: X-ray diffraction spectrum

The peaks have been fitted with a psudo-voigt model and a linear background around each peak, omitting the peaks around 0.9-1.0 rad that are due to the substrate and not the nanoparticles. Assuming a FCC structure, the peaks have been assigned to their respective Miller indices (l,m,n) and an estimation of the lattice constant has been obtained from each peak from the Bragg condition

$$2dsin(\theta) = \lambda \qquad\qquad d = \frac{a}{\sqrt{l^2 + m^2 + n^2}}$$

An estimation of the nanoparticles size has been obtained using the FWHM from the fit and the Scherrer formula (K = 0.89,$\beta_{inst} = 0.27°$)

$$D_V = K\frac{\lambda}{\beta_D cos(\theta)} \qquad\qquad \beta_D = \sqrt{\beta_{obs}^2 - \beta_{inst}^2}$$

In Tab.1 the obtained results are reported.

| Miller indices | (1,1,1) | (2,0,0) | (2,2,0) | (3,1,1) | (2,2,2) |
|---|---|---|---|---|---|
| Position(rad) | 0.668 | 0.776 | 1.131 | 1.357 | 1.429 |
| FWHM(rad) | 0.0134 | 0.0212 | 0.0160 | 0.0211 | 0.0192 |
| Lattice constant(nm) | 0.4069 | 0.4074 | 0.4067 | 0.4071 | 0.4071 |
| D(nm) | 9.83 | 6.82 | 9.75 | 8.14 | 9.19 |

Table 1: X-ray diffraction results

The values of the lattice constant are compatible and their mean has been taken as the final estimation

$$a = (0.4070 \pm 0.0001)nm$$

that is compatible with the bulk value of $a_{bulk} = 0.4065nm$. Even though the lattice constant is size dependent, the effect on particles of this dimensions is negligible as expected (*Size and shape dependent lattice parameters of metallic nanoparticles*[Weihong Qi,2005]).

The final estimation of the diameter has been taken as the mean of the values estimated from each peak, weighted by the area of the corresponding peak.

$$D = (8.9 \pm 0.3)nm$$

It is possible to see a significative discrepancy between the value obtained from the (2,0,0) peak and the rest, this has partly been attributed to the influence of the scattering on the Si substrate that also generates the peaks in the region [0.85;1] rad and that may contribute to the widening of the peak.

In general the estimations of the diameters obtained from this analysis are quite different. This has been attributed to the difference in the way the crystal planes responsible for the generation of these peaks are affected by the shape of the crystals (not completely spherical) and the effects due to the strain.

# 4 SEM

Particles are then observed using a scanning electron microscope. The nanoparticles are deposited over a silicon sample holder, and then inserted into the microscope chamber, where vacuum is created. A 10keV beam of electrons hit the sample, interacting in different ways with nanoparticles. In particular, secondary electrons backscattered are focused by a complex system of magnetic fields and collected by the in-lens detector. The acquired signal is an instantaneous picture of the nanoparticles, and permit to measure their properties. The contrast is due to atomic numbers and work functions of gold and silicon; the yield of backscattered electrons is higher for gold than for silicon, resulting in lighter area in correspondence of nanoparticles.

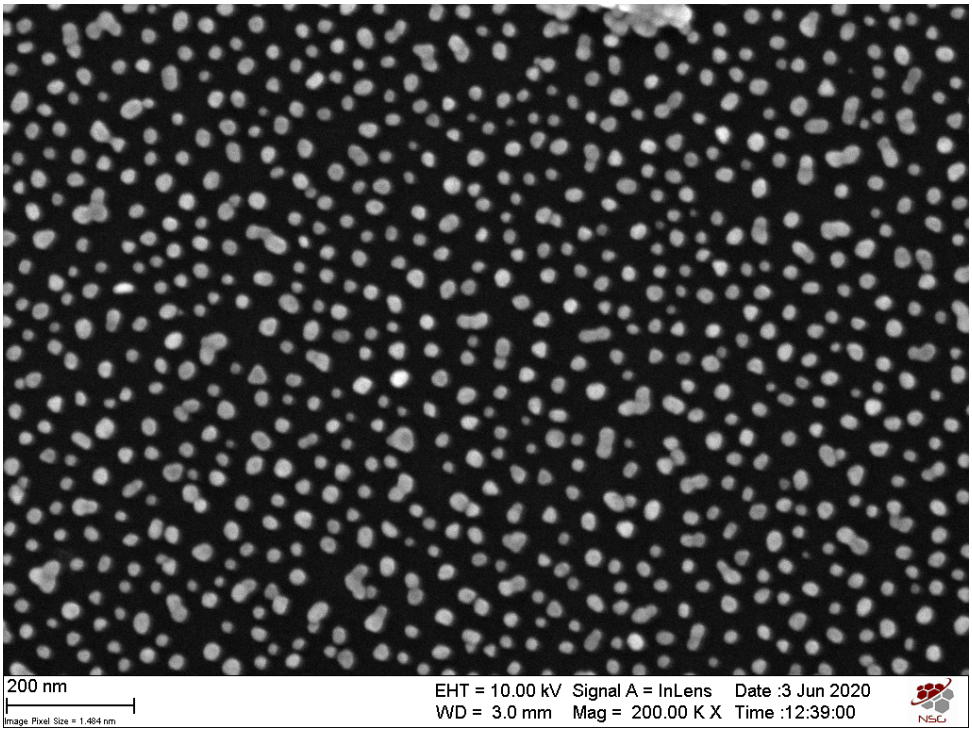


Figure 5: Image from SEM

To ensure a wide-enough statistic and properly estimated particle radius, between the various acquired picture the larger one (i.e. the one with minimum magnification) is chosen. The picture is analyzed, searching for all particles: a threshold is set, distinguishing gold from background, and for each particle the area is computed. Then, considering spherical approximation and the circle area $A = \pi R^2$, for each particle an effective radius is computed.

The distribution of radius is reported in fig. 6: neglecting the smallest values, due to errors and noise, and the greatest ones, due to multiple-nanoparticles clusters, the distribution is fitted with a log-normal one.

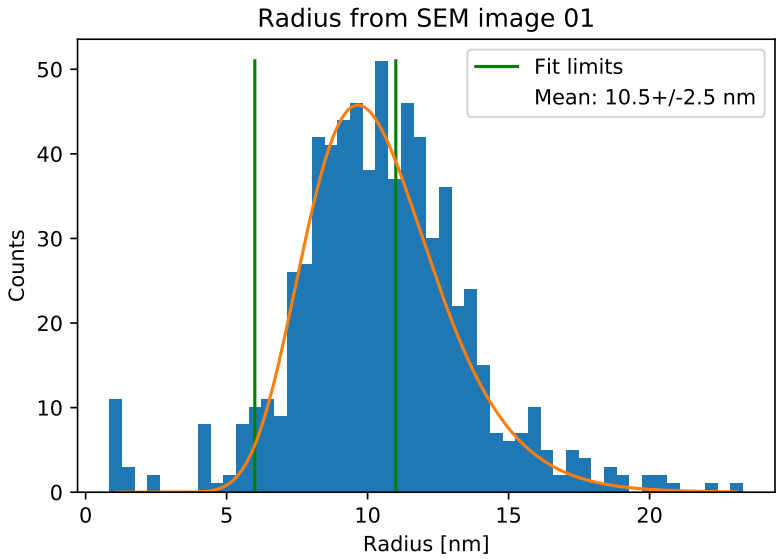


Figure 6: Radius of the particles

From the fit, an estimation of mean particle radius can be carried out:

$$\langle R \rangle = (11 \pm 3)\text{nm}$$
$$\langle R \rangle_V = (11 \pm 3)\text{nm}$$

where the subscript $V$ signals a mean weighted on nanoparticles volume, for a better comparison with XRay spectroscopy results. While this result confirm the order of magnitude found from optical absorption spectrum, it's clear that it is not compatible with the Xray one.

From the SEM images, also eccentricity studies can be carried out. Using a more magnified picture of the nanoparticles, their shape is observed and the eccentricity calculated. The results are reported in the following figures.

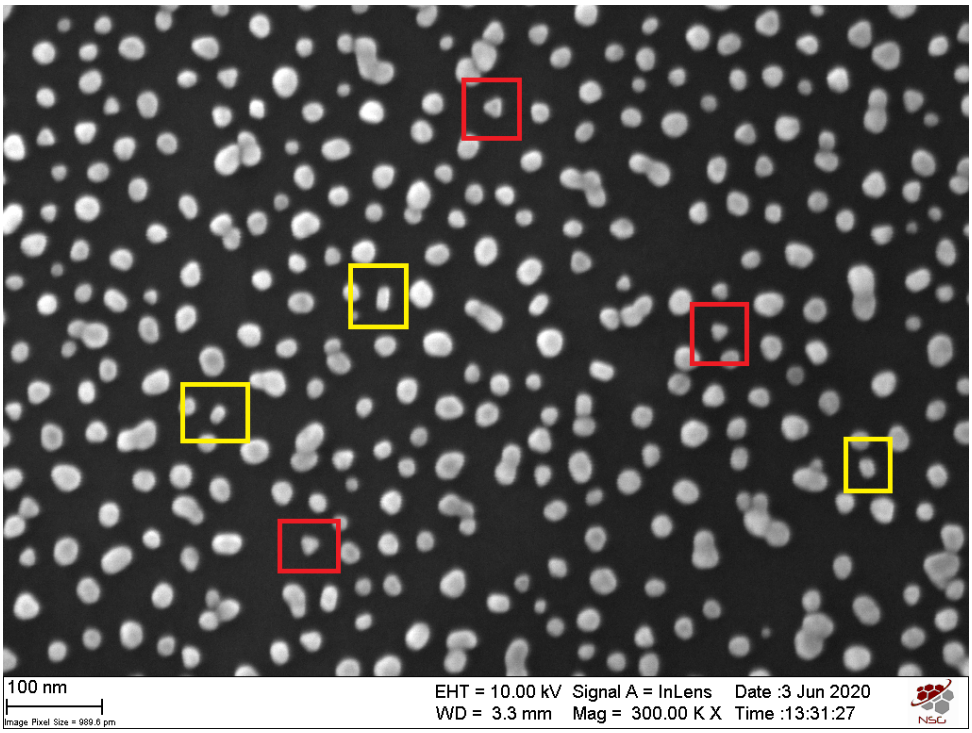


Figure 7: Image from SEM. Some particularly shaped particles has been highlighted: triangular ones (red) and strongly-elliptic ones (yellow)

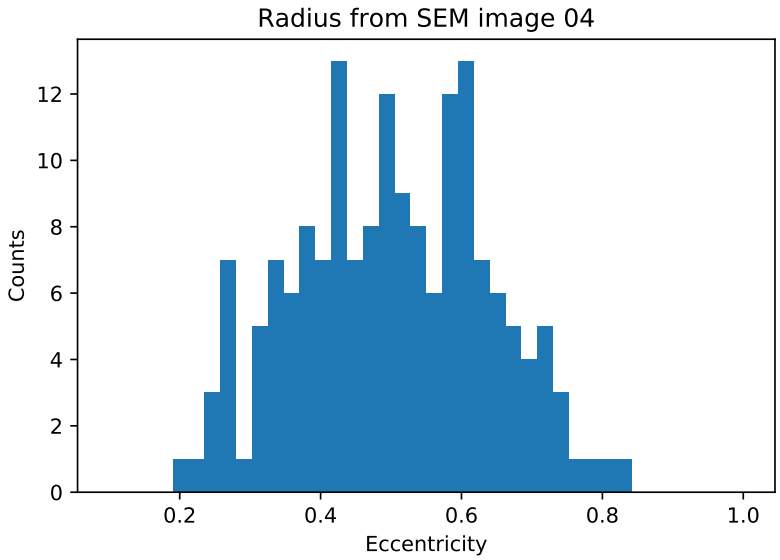


Figure 8: Eccentricity of particles in fig. 7, escluding biggest and smaller ones as in fig. 6

As can be seen from the plot in fig. 7, there is a wide range of different cell eccentricities. This can be one of the main issues which distort our previous estimation form X-ray diffraction. In fact, eccentricity affect peaks broadening; in computing estimated diameters from XRay peaks FWHM, we neglected this contribute, that if considered contribute in lowering $\beta_D$ and therefore rising the estimation of diameter.

## 5 EDS

Through the SEM, it's also possible to perform an X-Ray spectroscopy of the sample. Selecting a wide nanoparticles cluster, the x-rays emitted as a de-excitation process in the sample can be measured and their intensity as a function of the energy can be analyzed. The positions of the peaks are strongly correlated to the elements of which the sample is made of; comparing the measured spectra with the known peaks of xray emission, it's clear that the sample is made of silicon (i.e., the material of the sample holder) and gold, confirming the nature of our nanoparticles.

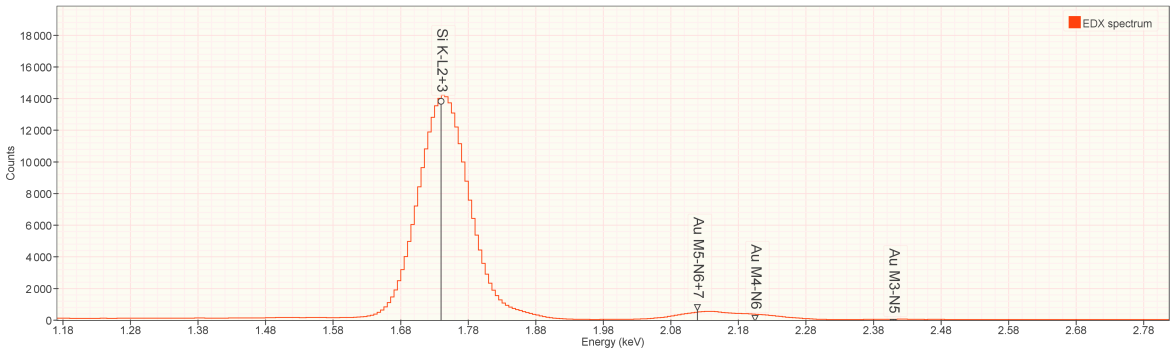


Figure 9: Composition of the Nanoparticles

## 6 Optical and XRay spectra simulation

A simulation script is used to compare the measured absorption spectrum with the one that can be obtained from theoretical predictions. In Fig. 10 it is possible to see the simulated near-field properties of a gold nanoparticle of R = 10 nm for a planar incident wave travelling in the z direction and polarized

along the x axis in a medium with n=1.4. The images are taken by sectioning perpendicularly to the z axis in correspondence to the center of the particle.

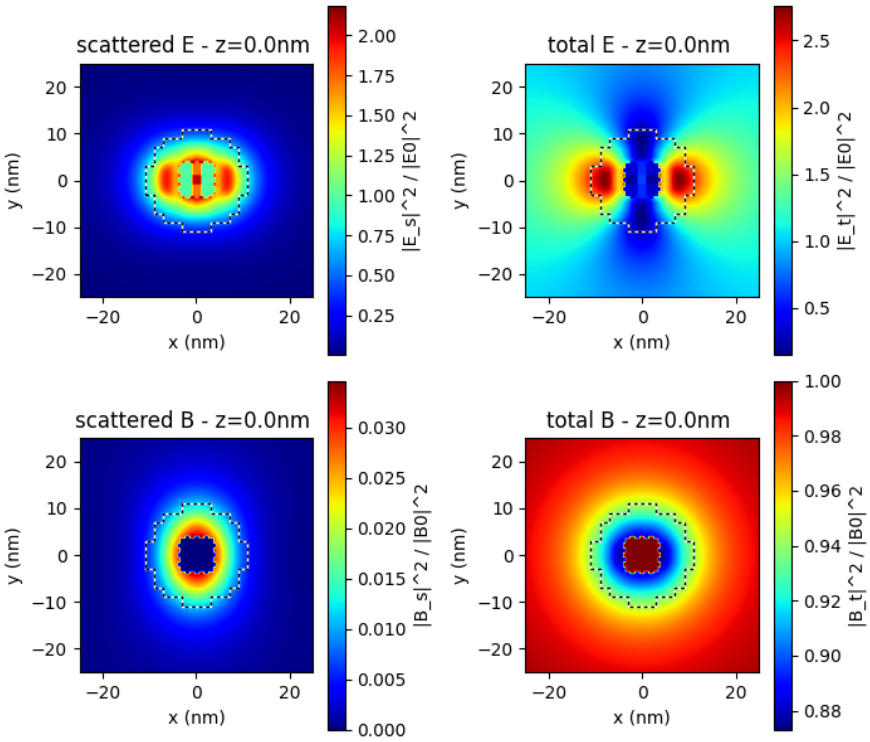


Figure 10: Simulated near-field

In Fig.11 the spectrum corresponding to the absorbance is compared to the one obtained experimentally. The simulated spectra shows a peak in the expected position and the differences are attributed to the size distribution of the particles and to the non-spherical shape, but the agreement is still considered acceptable.

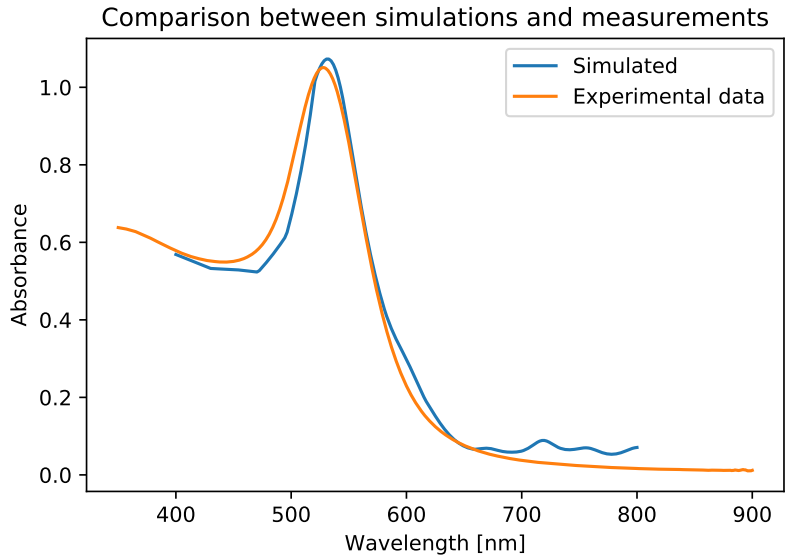


Figure 11: Simulated Cross sections

## Conclusions

In this report, an analysis of gold nanoparticles has been carried out. Firstly, measuring the absorption spectrum in visible wavelengths, an estimation of the orders of magnitude of density, radius and medium dielectric function have been obtained; the big uncertainties on the size equation coefficient didn't allow to obtain more quantitative predictions. However, these results confirm us the legitimacy of the non-interacting approximation.

Through X-ray diffraction measures, a more quantitative estimation of nanoparticles diameters has been obtained; unfortunately, this results has been proved wrong from succeeding measurements, probably due to eccentricity and strain effects.

Then, nanoparticles has been observed through a scanning electron microscope; from the collected pictures, estimations of nanoparticles diameters and eccentricities have been obtained. It has been observed a wide distribution of both diameters and eccentricity, showing a strongly non-uniform system.

Finally, two additional analysis has been carried out; one regarding nanoparticles composition, through X-Ray spectroscopy, confirming gold nanoparticles and silicon holder; the other comparing simulations and measurements of optical absorption spectrum, showing coherence of oue dataset.

The most valuable results are, clearly, the one from SEM pictures, in which nanoparticles are directly observed.